

# Multi-Carrier $M$ -ary DCSK System with Code Index Modulation: An Efficient Solution for Chaotic Communications

Guofa Cai, *Member, IEEE*, Yi Fang, *Member, IEEE*, Jinming Wen, Shahid Mumtaz, *Senior Member, IEEE*, Yang Song, and Valerio Frascolla

**Abstract**—A new multi-carrier  $M$ -ary differential chaos shift keying system with code index modulation, referred to as *CIM-MC-M-DCSK*, is proposed in this paper. In the proposed *CIM-MC-M-DCSK* system, the reference and information-bearing signals for each subcarrier can be transmitted simultaneously by using the orthogonal sinusoidal carriers, where the information-bearing signal adopts the  $M$ -DCSK modulation to further increase the data rate. With an aim to making full use of the system energy resources, the reference signals in all subcarriers are coded by a Walsh code to carry additional information bits. The analytical bit-error-rate (BER) expressions of the proposed *CIM-MC-M-DCSK* system are derived over additive white Gaussian noise (AWGN) as well as multipath Rayleigh fading channels. Furthermore, a noise-reduction scheme and a hierarchical-modulation scheme are designed for the proposed system. In particular, the former scheme can significantly improve the BER performance while the latter scheme can provide different quality of service (QoS) for the transmitted bits according to their different levels of importance. Simulation results verify the accuracy of the analytical expressions and the superiority of the proposed systems.

**Index Terms**—Code index modulation; Multi-carrier  $M$ -ary DCSK; Bit error rate; AWGN channel; Multipath Rayleigh fading channel.

## I. INTRODUCTION

This work was partially supported by National Natural Science Foundation of China (Nos. 61701121, 61771149, 11871248, 61801128), the Open Research Fund of State Key Laboratory of Integrated Services Networks under Grant ISN19-04, the Guangdong Province Universities and Colleges Pearl River Scholar Funded Scheme under Grant 2017-ZJ022, the NSF of Guangdong Province under Grant 2016A030310337, the Special Innovation Project of the Education Department of Guangdong Province under Grant 2017KTSCX060, the Fundamental Research Funds for the Central Universities under Grant 21618329, and the Project of Department of Education of Guangdong Province (Nos. 2018XSLT13, 2018SFJD-01), the Fundamental Research Funds for the Central Universities (No. 21618329), the European Union's Horizon 2020 research and innovation programme under grant agreement (No. 815178), and the Science and Technology Program of Guangzhou, China (No. 201802020007). (*Corresponding author: Yi Fang.*)

G. Cai and Y. Fang are with the School of Information Engineering, Guangdong University of Technology, Guangzhou 510006, China, and also with the State Key Laboratory of Integrated Services Networks, Xidian University, Xi'an 710126, China (e-mail: {caiguofa2006, fangyi}@gdut.edu.cn).

J. Wen is with the College of Information Science and Technology and the College of Cyber Security, Jinan University, Guangzhou 510632, China (e-mail: jinming.wen@mail.mcgill.ca).

S. Mumtaz is with the Institute of Telecommunications, 1049-001 Aveiro, Portugal (e-mail: smumtaz@av.it.pt).

Y. Song is with the School of Electrical and Electronic Engineering, Nanyang Technological University, Singapore 639798 (e-mail: songy@ntu.edu.sg).

V. Frascolla is with Intel Deutschland GmbH, Neubiberg 85579, Germany (e-mail: valerio.frascolla@intel.com).

**D**IFFERENTIAL chaos shift keying (DCSK) system can not only achieve excellent performance over multipath fading or time-varying channels, but also be amenable to low-complexity implementation [1]. In the past decade, the performance of the DCSK system has been studied in various communication scenarios, e.g., ultra-wideband applications [2], two-way relay network-coded system [3], simultaneous wireless information and power transfer system [4], continuous mobility communication system [5], power line communication system [6], cooperative scheme [7], coexisting communication system [8], and multiple input multiple output system [9]. Owing to the inherent low-cost and anti-multipath-fading properties, the DCSK system can be considered as promising candidate for low-complexity and low-power short-range wireless-communication applications, e.g., wireless sensor networks and wireless body area networks.

In the conventional DCSK system, a half of the symbol energy is used to transmit the reference signal, thus resulting in relatively low energy efficiency and data rate. To improve data rate and increase energy efficiency, an orthogonal multilevel DCSK system has been proposed by constructing a set of orthogonal chaotic signal [10]. Based on quadrature chaotic shift keying [11], a generalized constellation-based  $M$ -ary DCSK ( $M$ -DCSK) system framework has been conceived to obtain high data rate [12]. Moreover, the data rate and energy efficiency of the DCSK system can be further improved through optimizing the length of reference signal [13]. On the other hand, to satisfy different quality of service (QoS) requirements, two hierarchical  $M$ -DCSK modulations, i.e., multiresolution circle-constellation-based  $M$ -DCSK (MR- $M$ -DCSK) [14] and hierarchical square-constellation-based  $M$ -DCSK systems [15], have been designed by exploiting the non-uniformly spaced constellations. More recently, an adaptive MR- $M$ -DCSK system has been conceived by adjusting the constellation parameter so as to accomplish a more flexible error performance [16]. Besides, to mitigate the negative effect of channel noise, a noise-reduction DCSK system [17] has been developed by sending and averaging multiple replicas of the reference signal [18], [19].

The conventional DCSK system includes many radio-frequency (RF) delay lines, which are extremely difficult to be implemented. To remove the RF delay lines at the receiver, a Walsh-code-based code-shifted DCSK system has been proposed in [20], [21]. As a further advancement, a multi-carrier DCSK (MC-DCSK) system has been developed

by allocating different frequency carriers to the reference and information-bearing signals [22]. As compared with the conventional DCSK system, the MC-DCSK system not only avoids the use of RF delay lines but also enhances the energy efficiency and data rate. Following this work, a multiuser MC-DCSK system has been further designed in [23] so as to satisfy the requirements of practical wireless-communication applications. As an alternative, the delay lines can be avoided by using the orthogonal sinusoidal carriers. Therefore, an orthogonal-sinusoidal-carrier-based DCSK system has been conceived in [24], which can achieve a doubled data rate compared with the conventional DCSK system.

Alternatively, index modulation is another desirable solution to increase the data rate and to save energy [25]-[32]. In recent years, the joint design of index modulation and spread spectrum has been carefully investigated so as to explore more potential benefits from the data-rate and energy-efficiency perspectives [33], [34]. In [35], [36], spatial modulation has been applied to DCSK system to increase the data rate, where the antenna index is used to convey additional information bits. In [37], [38], [39], code-index-modulation (CIM) DCSK schemes, which select different Walsh codes to convey additional information bits, have been proposed to increase the data rate and to enhance energy efficiency. Moreover, a permutation-matrix-based permutation-index DCSK system, which is able to not only achieve multi-user high-data-rate transmission but also enhance system security, has been introduced in [40]. In addition, a carrier-index MC-DCSK system has been conceived to further reduce the system complexity and remove all RF delay lines [41]. In particular, the subcarrier index in the carrier-index MC-DCSK system are exploited to convey additional information bits. Aiming at further boosting the data rate, the carrier-index MC-DCSK system has been extended to  $M$ -ary domain, and thus formulating two carrier-index MC- $M$ -DCSK schemes [42].

Inspired by CIM and MC- $M$ -DCSK modulations, we propose in this paper a new CIM-MC- $M$ -DCSK communication system. In the proposed system, the orthogonal sinusoidal carriers are used to simultaneously transmit the reference and the information-bearing signals for each subcarrier. Specifically, the  $M$ -DCSK modulation is adopted in each information-bearing signal while the reference signals in all subcarriers are coded by a Walsh code. The proposed CIM-MC- $M$ -DCSK system not only inherits the low-complexity advantage of the MC-DCSK system, but also has a higher data rate and achieves a better performance thanks to the Walsh-codes-based index modulation. Moreover, the analytical bit-error-rate (BER) expressions of the proposed CIM-MC- $M$ -DCSK system are derived over additive white Gaussian noise (AWGN) as well as multipath Rayleigh fading channels. Besides, a noise-reduction scheme and a new hierarchical-modulation scheme are designed for the proposed system to further improve the error performance and QoS, respectively. Last but not the least, the simulation results are highly consistent with the analytical BER results, both of which illustrate that the proposed CIM-MC- $M$ -DCSK system and its hierarchical-modulation system significantly outperforms the conventional MC- $M$ -DCSK system and its corresponding hierarchical-modulation

one, respectively. In summary. The main contributions of this paper are as follows:

- 1) A new MC- $M$ -DCSK with code index modulation system, referred to as *CIM-MC- $M$ -DCSK system*, is proposed, where the code index modulation and the  $M$ -DCSK modulation are used in the reference signals and information-bearing signals, respectively.
- 2) A noise-reduction scheme and a hierarchical-modulation scheme are designed and tailored for the proposed CIM-MC- $M$ -DCSK system. In particular, the noise-reduction scheme significantly improves the BER performance while the hierarchical-modulation scheme can provide more flexible QoS for different transmitted bits according to their different importance levels.
- 3) The analytical BER expressions of the proposed CIM-MC- $M$ -DCSK system are derived over AWGN and multipath Rayleigh fading channels. Moreover, various simulations are performed to validate the accuracy of the theoretical analysis and the advantages of the proposed system.

The remainder of this paper is organized as follows. Section II gives the proposed system model. Section III derives the analytical BER performance of the proposed system. The noise-reduction and hierarchical-modulation schemes of the proposed system are proposed in Section IV. Numerical results and discussions are shown in Section V. Section VI concludes the paper.

## II. SYSTEM MODEL

### A. Transmitter of the Proposed System

The block diagram of the proposed CIM-MC- $M$ -DCSK system is shown in Fig. 1. In the CIM-MC- $M$ -DCSK system, an  $M$ -DCSK modulation is used in the information-bearing signal for each subcarrier while the code index modulation is applied to the reference signals. Moreover, to ensure their orthogonal transmission, the orthogonal sinusoidal carriers are adopted in both the reference signals and information-bearing signals. In this paper, the reference signal is referred to as the in-phase baseband signal while the information-bearing signal is referred to as the quadrature baseband signal.

At the transmitter as shown in Fig. 1(a), the serial information sequences are first converted into  $N+1$  parallel sequences by using a serial-to-parallel converter, where each parallel sequence is denoted by  $b_i$  ( $i = 0, 1, \dots, N$ ),  $N = 2^n$ , and  $n$  is the number of transmitted bits by using the  $N$ -order Walsh codes. The index bits  $b_0$  and modulated bits  $b_i$  are converted into a symbol  $S_0$  and a symbol  $S_i$  by using an  $N$ -ary and  $M$ -ary bit-to-symbol converter, respectively, where  $S_0 \in \{0, 1, \dots, N-1\}$  and  $S_i \in \{0, 1, \dots, M-1\}$ . Second, the chaotic generator adopts a second-order Chebyshev polynomial function, i.e.,  $x_{k+1} = 1 - 2x_k^2$ , to generate a chaotic signal  $c_x = (c_{x,1}, \dots, c_{x,\beta})$  with a spreading factor  $\beta$  and a chip duration  $T_c$ . The chaotic signal  $c_x$  is transformed into another orthogonal chaotic signal  $c_y = (c_{y,1}, \dots, c_{y,\beta})$  by using a Hilbert filter, where  $\sum_{i=1}^{\beta} c_{x,i}c_{y,i} = 0$ . For the  $i$ -th quadrature subcarrier, the quadrature baseband signal can be obtained as  $m_{S_i} = a_{S_i}c_x + b_{S_i}c_y$  by using the  $M$ -DCSK

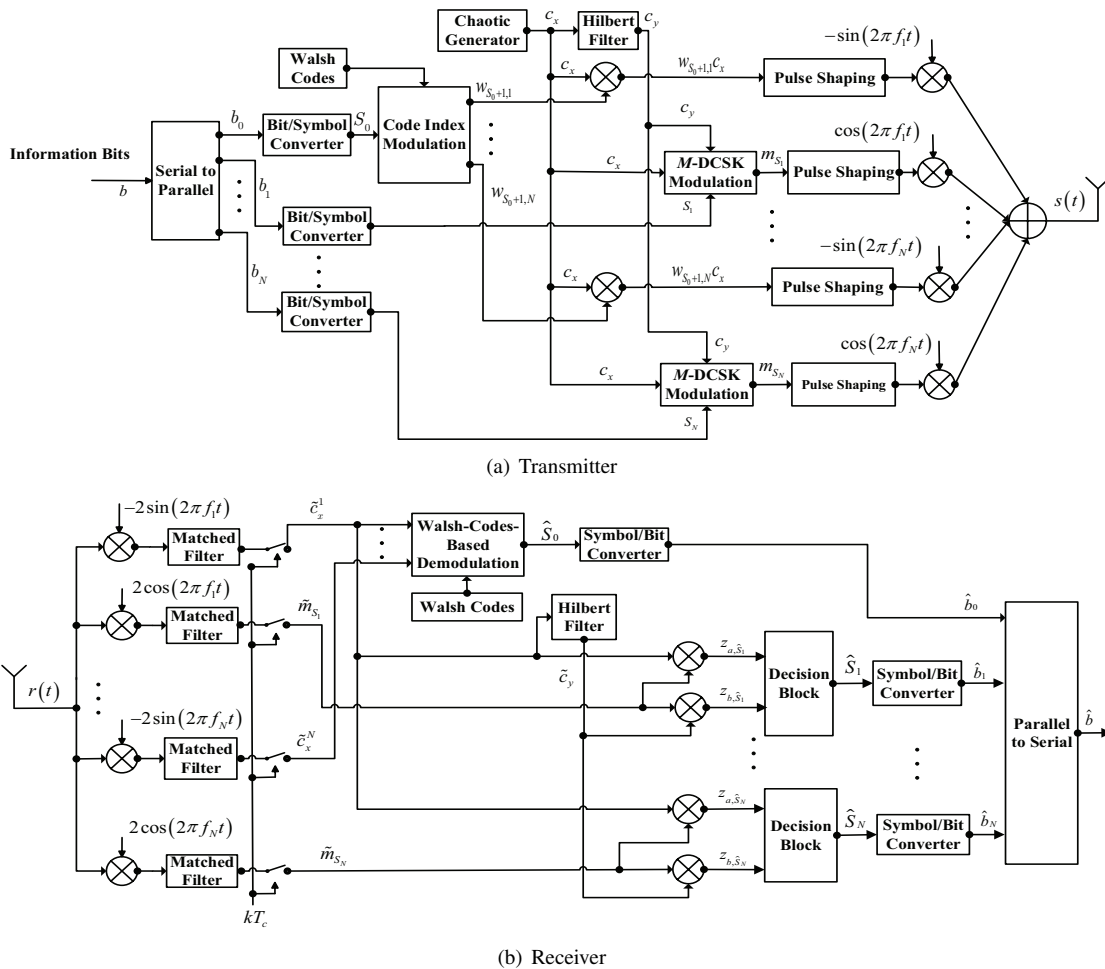


Fig. 1. The block diagram of a CIM-MC-M-DCSK system.

modulation, where  $a_{S_i}$  and  $b_{S_i}$  are regenerated via an  $M$ -DCSK constellation. For example, Fig. 2 shows a generalized 8-DCSK constellation, where the constellation points are controlled by the angle vector  $\theta = [\pi/2 - \theta_1, \theta_2, \dots, \theta_{m-1}]$  and  $m = 3$ .<sup>1</sup> As a special case, the angle vector of a uniform 8-DCSK constellation equals  $\theta = [\pi/4, \pi/8]$ .

Third, a code index modulation is used for all the in-phase subcarriers. More specifically, the chaotic signals  $c_x$  for all in-phase subcarriers are encoded by an  $N$ -order Walsh code, where the Walsh code is defined as  $W_{2^n} = \begin{bmatrix} W_{2^{n-1}} & W_{2^{n-1}} \\ W_{2^{n-1}} & -W_{2^{n-1}} \end{bmatrix}$  and  $W_{2^0} = [+1]$ , for  $N = 2^n$ ,  $n \geq 1$ . For a given  $S_0$ , the  $(S_0 + 1)$ -th row of the Walsh code matrix, i.e.,  $w_{S_0+1} = [w_{S_0+1,1}, \dots, w_{S_0+1,i}, \dots, w_{S_0+1,N}]$ , is used to transmit the information for in-phase subcarrier, thus the in-phase baseband signal is written as  $w_{S_0+1}^T c_x$ , e.g., for the  $i$ -th subcarrier one has  $w_{S_0+1,i} c_x$ , where  $(\cdot)^T$  denotes the transpose of a matrix or a vector. Finally, the in-phase and quadrature baseband signals are passed through the pulse shaping with a square-root-raised-cosine filter  $q(t)$ . The in-phase and quadrature

<sup>1</sup>Although the square-based constellations can be used in this paper, partial channel state information (CSI) and high peak-to-average-power ratio (PAPR) are required [12], [15]. To meet the requirements of low-complexity short-range wireless-communication applications, in this paper the circle-based constellations are adopted because they require no CSI and have low PAPR [14].

ture signal components are  $x_{I,i}(t) = \sum_{k=1}^{\beta} m_{S_i,k} q(t - kT_c)$  and  $x_{Q,i}(t) = \sum_{k=1}^{\beta} w_{S_0+1,i} c_{x,k} q(t - kT_c)$ , respectively. Therefore, as shown in Fig. 1, the transmitted signal of the CIM-MC-M-DCSK system can be expressed as

$$s(t) = \sum_{i=1}^N \left( x_{I,i}(t) \cos(2\pi f_i t) - x_{Q,i}(t) \sin(2\pi f_i t) \right), \quad (1)$$

where  $f_i$  is the frequency of the sinusoidal carrier satisfying  $f_i \gg 1/T_c$ , and any two frequencies, i.e.,  $f_i$  and  $f_j$  ( $i \neq j$ ), must be mutually orthogonal.

The transmitted signal is passed through a multipath fading channel  $h(t) = \sum_{l=1}^L \alpha_l \delta(t - \tau_l)$ , where  $L$  is the number of paths,  $\alpha_l$  and  $\tau_l$  are the channel coefficient and the path delay of the  $l$ -th path, respectively, and  $\otimes$  is the convolution operator. In addition, in this paper we assume that  $\alpha_l$  ( $l = 0, \dots, L$ ) are independent Rayleigh distribution random variables. Hence, the received signal is given by

$$r(t) = h(t) \otimes s(t) + n(t), \quad (2)$$

where  $n(t)$  is the AWGN with zero mean and variance of  $N_0/2$ .

### B. Receiver of the Proposed System

At the receiver as shown in Fig. 1(b), the received signal  $r(t)$  is first processed by the in-phase and quadrature car-

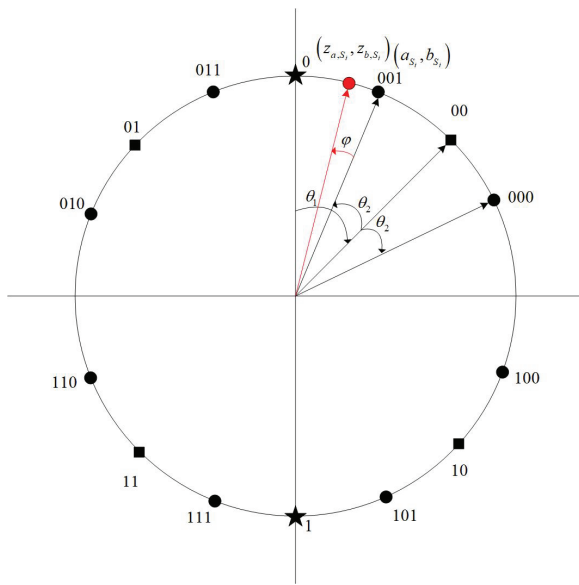


Fig. 2. A generalized 8-DCSK constellation.

riers and the matched filters, then one obtains the in-phase and quadrature baseband signals. For example, for the  $i$ -th subcarrier one has  $\tilde{c}_x^i$  and  $\tilde{m}_{S_i}$ . It should be noted that the first component for any row of the Walsh code matrix is  $+1$ . It is evident that the in-phase baseband signal corresponding to the frequency  $f_1$  can be used as the reference signal. This reference signal is adopted to demodulate the quadrature baseband signals. Hence, the Walsh-codes-based demodulation and  $M$ -DCSK demodulation can be simultaneously performed.<sup>2</sup> Specifically, the energy detection is deployed in Walsh-codes-based demodulation while the differentially coherent detection is adopted in the  $M$ -DCSK demodulation.

When demodulating either the CIM or  $M$ -DCSK, a simple product operation for the two matrices or vectors is performed. For the demodulation of the CIM, the following expression is first computed:  $A = [w_1, \dots, w_N]^T \times [\tilde{c}_x^1, \dots, \tilde{c}_x^N]^T$ . Then, energy vector  $z_e = [z_{e,1}, \dots, z_{e,\hat{S}_0+1}, \dots, z_{e,N}]$  is obtained by computing the energy value for any row of the matrix  $A$ . Hence, the symbol  $S_0$  can be estimated using

$$\hat{S}_0 = \arg \max_{i=1, \dots, N} (z_{e,i}) - 1. \quad (3)$$

For the demodulation of  $M$ -DCSK, the reference baseband signal  $\tilde{c}_x^1$  is transformed into another orthogonal reference signal  $\tilde{c}_y$  by using a Hilbert filter. Afterwards, the two decision values for the  $i$ -th subcarrier, i.e.,  $z_{a,\hat{S}_i} = \tilde{c}_x^1 \tilde{m}_{S_i}^T$  and  $z_{b,\hat{S}_i} = \tilde{c}_y \tilde{m}_{S_i}^T$ , can be measured. We refer to  $z_i = (z_{a,\hat{S}_i}, z_{b,\hat{S}_i})$  as the decision vector. Further, one can calculate the distance between the decision vector and all constellation points, and thus find the position of the minimum distance corresponding to the constellation point. Hence, the estimated symbol  $\hat{S}_i$  for the  $i$ -th subcarrier is obtained. The estimated symbols are converted into the estimated bits by using the symbol-to-bit

<sup>2</sup>In the proposed CIM-MC- $M$ -DCSK system, because the detections of the code-index modulation and  $M$ -DCSK modulation are independent of each other, the error detection of the code-index modulation does not affect the demodulation performance of the  $M$ -DCSK modulation.

converter. Finally, all the parallel bits, i.e.,  $\hat{b}_0, \dots, \hat{b}_N$ , are converted into the serial bits  $\hat{b}$  via a parallel-to-serial converter.

### III. PERFORMANCE ANALYSIS

In this section, we derive the analytical BER expressions of the proposed system over AWGN and multipath Rayleigh fading channels.

#### A. Bit Energy

Since the energy of a chaotic signal  $c_x$  is expressed by  $E_1 = \sum_{k=1}^{\beta} c_{x,k}^2$ , the total energy of the proposed system equals  $E_{tot} = 2NE_1$ . Moreover, the number of the transmitted bits is

$$R = \log_2 N + N \log_2 M, \quad (4)$$

As a result, the average transmitted energy of each bit, i.e.,  $E_b$ , is given as

$$E_b = \frac{E_{tot}}{R} = \frac{2NE_1}{\log_2 N + N \log_2 M}. \quad (5)$$

#### B. Derivation of Probability Density Functions (PDFs)

In this paper, we assume that the largest multipath delay  $\tau_L$  is much shorter than the symbol duration, i.e.,  $0 < \tau_L \ll \beta$ , thus the inter-symbol interference (ISI) can be negligible [8], [10], [13], [14]. Also, we assume that the channel is slowly fading and the channel coefficients are constant during each symbol duration but varies from symbol to symbol.<sup>3</sup>

For the Walsh-code-based demodulation of the CIM, the  $j$ -th ( $j = 1, 2, \dots, N$ ) energy metric can be written as

$$z_{e,j} = \left[ \sum_{i=1}^N \sum_{k=1}^{\beta} \left( \sum_{l=1}^L \alpha_l w_{j,i} w_{S_0+1,i} c_{x-\tau_l} + w_{j,i} n_{x,k}^i \right) \right]^2, \quad (6)$$

where  $n_x^i$  denotes the AWGN for the  $i$ -th subcarrier.

If  $j = S_0 + 1$ , the energy metric is computed as

$$z_{e,j} = \left[ \sum_{k=1}^{\beta} \left( N \sum_{l=1}^L \alpha_l c_{x-\tau_l} + \sum_{i=1}^N w_{j,i} n_{x,k}^i \right) \right]^2. \quad (7)$$

Otherwise, if  $j \neq S_0 + 1$ , the energy metric is calculated as

$$z_{e,j} = \left( \sum_{k=1}^{\beta} \sum_{i=1}^N w_{j,i} n_{x,k}^i \right)^2. \quad (8)$$

Accordingly, all the elements in the energy vector  $z_e = [z_{e,1}, \dots, z_{e,j}, \dots, z_{e,N}]$  are mutually independent. When the transmitted symbol  $S_0$  equals  $j - 1$ ,  $z_{e,j}$  is a non-central chi-square random variable with  $\beta$  degrees of freedom and non-centrality parameter  $NE_1 \sum_{l=1}^L \alpha_l^2$ , while  $z_{e,i}$  ( $i \neq j$ ) is central chi-square random variables with  $\beta$  degrees of freedom. In addition, the noise variance of all the elements in the vector  $z_e$  can be obtained as  $NN_0/2$ . Hence, the

<sup>3</sup>Although the investigation of the effect of the carrier frequency offset (CFO) and time-varying channels on BER performance of the proposed system is an interesting topic, it is beyond the scope of this paper. We will explore this issue in the future.

instantaneous PDFs of  $z_{e,j}$  and  $z_{e,i}$  conditioned on the bit signal-to-noise ratio (SNR)  $\gamma_b$  respectively become

$$p(z_{e,j}|\gamma_b) = \frac{1}{NN_0} \times \left( \frac{z_{e,j}}{NE_1 \sum_{l=1}^L \alpha_l^2} \right)^{\frac{\beta-2}{4}} \times \exp\left(-\frac{NE_1 \sum_{l=1}^L \alpha_l^2 + z_{e,j}}{NN_0}\right) \times I_{\left(\frac{\beta}{2}-1\right)}\left(\frac{2\sqrt{z_{e,j}NE_1 \sum_{l=1}^L \alpha_l^2}}{NN_0}\right), \quad (9)$$

$$p(z_{e,i}|\gamma_b) = \frac{z_{e,i}^{\frac{\beta}{2}-1}}{(NN_0)^{\frac{\beta}{2}} \Gamma\left(\frac{\beta}{2}\right)} \exp\left(-\frac{z_{e,i}}{NN_0}\right), \quad (10)$$

where  $\gamma_b = \left(\sum_{l=1}^L \alpha_l^2\right) (E_b/N_0)$ ,  $z_{e,j} \geq 0$ ,  $z_{e,i} \geq 0$ ,  $i \neq j$ ,  $I_{(n)}(\cdot)$  denotes the  $n$ -th Bessel function of the first kind and  $\Gamma(\cdot)$  presents the Gamma functions.

For  $M$ -DCSK modulation, one can obtain the means and the variances of the vector  $z_i$  for the  $i$ -th subcarrier according to [14],  $E[z_{a,\hat{s}_i}] = a_{S_i} E_1 \sum_{l=1}^L \alpha_l^2$ ,  $E[z_{b,\hat{s}_i}] = b_{S_i} E_1 \sum_{l=1}^L \alpha_l^2$ , and  $Var[z_{a,\hat{s}_i}] = Var[z_{b,\hat{s}_i}] = E_1 N_0 \sum_{l=1}^L \alpha_l^2 + \frac{\beta N_0^2}{4}$ , respectively, where  $E[\cdot]$  and  $Var[\cdot]$  denote the expectation and variance operators, respectively. Through the polar coordinates transformations of the energy vector  $z_i$  for the  $i$ -th subcarrier and some simplified computations, the instantaneous PDF conditioned on  $\gamma_b$  is calculated as

$$p(\varphi|\gamma_b) = \frac{1}{2\pi} \exp\left(\frac{-\gamma^2}{8}\right) + \frac{\gamma \cos \varphi}{2\sqrt{2\pi}} \times \exp\left(\frac{-\gamma^2 \sin^2 \varphi}{8}\right) \times Q\left(\frac{-\gamma \cos \varphi}{2}\right), \quad (11)$$

where  $\varphi$  denotes the phase error between the transmitted and the received signal constellations as shown in Fig. 2,  $Q(x) = \frac{1}{\sqrt{2\pi}} \int_x^\infty \exp\left(-\frac{t^2}{2}\right) dt$ , and the parameter  $\gamma$  is calculated as

$$\gamma = \frac{\frac{2R}{N} \gamma_b}{\sqrt{\frac{2R}{N} \gamma_b + \beta}}. \quad (12)$$

### C. Derivation of BER Expressions

According to the principle of the orthogonal modulation in [43], the probability of incorrect symbol detection for the Walsh-code-based index modulation can be obtained as  $P_{s,CIM}(\gamma_b) = 1 - \Pr(z_{e,i} < z_{e,j}, \forall i \neq j|\gamma_b)$ , where  $\Pr(\cdot)$  is the probability of correct symbol detection. Since the events of  $\Pr(\cdot)$  are not independent due to the existence of the random variable  $z_{e,j}$ , one can add a condition on  $z_{e,j}$  to make these events independent. In addition, one can easily find that the energy metric  $z_{e,k}$  ( $k = 1, 2, \dots, N$ ) is non-negative. Thereby, one has  $P_{s,CIM}(\gamma_b) = 1 - \int_0^\infty [\Pr(z_{e,i} < z_{e,j}|z_{e,j}, \gamma_b)]^{N-1} p(z_{e,i}|\gamma_b) dz_{e,j}$ . Using the PDFs in Eqs. (9) and (10), the symbol error rate (SER) expression of the Walsh-code-based index modulation can be

derived as

$$P_{s,CIM}(\gamma_b) = 1 - \int_0^\infty \left( \int_0^{z_{e,j}} \frac{z_{e,i}^{\frac{\beta}{2}-1} \exp\left(-\frac{z_{e,i}}{NN_0}\right)}{(NN_0)^{\frac{\beta}{2}} \Gamma\left(\frac{\beta}{2}\right)} dz_{e,i} \right)^{N-1} \times \left( \frac{z_{e,j}}{NE_1 \sum_{l=1}^L \alpha_l^2} \right)^{\frac{\beta-2}{4}} \frac{\exp\left(-\frac{NE_1 \sum_{l=1}^L \alpha_l^2 + z_{e,j}}{NN_0}\right)}{NN_0} \times I_{\left(\frac{\beta}{2}-1\right)}\left(\frac{2\sqrt{z_{e,j}NE_1 \sum_{l=1}^L \alpha_l^2}}{NN_0}\right) dz_{e,j}. \quad (13)$$

Let  $t = z_{e,i}/(NN_0/2)$  for  $i \neq j$  and  $u = z_{e,j}/(NN_0/2)$ , one can further simplify Eq. (13) to

$$P_{s,CIM}(\gamma_b) = \frac{1}{2} \int_0^\infty (1 - F(u)^{N-1}) \times \left(\frac{u}{R\gamma_b}\right)^{\frac{\beta-2}{4}} \times \exp\left(-\frac{R\gamma_b + u}{2}\right) \times I_{\left(\frac{\beta}{2}-1\right)}(\sqrt{uR\gamma_b}) du, \quad (14)$$

where  $F(u) = \int_0^u \frac{1}{2^{\frac{\beta}{2}} \Gamma\left(\frac{\beta}{2}\right)} t^{\frac{\beta}{2}-1} \exp(-t) dt$  and denotes the cumulative distribution function (CDF) of the central chi-square distribution. According to the theory of orthogonal signaling in [43, pp. 205], the BER expression of the Walsh-code-based index modulation can be given by

$$P_{b,CIM}(\gamma_b) = \frac{N}{2(N-1)} P_{s,CIM}(\gamma_b). \quad (15)$$

For  $M$ -DCSK modulation in the proposed system, the BER expression can be derived by using the PDF in the Eq. (11), i.e.,

$$P_{b,MDCSK}(\gamma_b) = \frac{1}{\log_2 M} \left(1 - \int_{-\frac{\pi}{M}}^{\frac{\pi}{M}} p(\varphi|\gamma_b) d\varphi\right). \quad (16)$$

In the high SNR region, one can obtain an approximated closed-form expression of Eq. (16), which is expressed as

$$P_{b,MDCSK}(\gamma_b) \approx \frac{2}{\log_2 M} Q\left(\frac{\gamma \sin\left(\frac{\pi}{M}\right)}{2}\right). \quad (17)$$

The detailed derivation of Eq. (17) can be found in Appendix.

In this paper, we make the assumption that the  $L$  paths of a multipath fading channel are mutually independent and have identical channel gains. Accordingly, the PDF of  $\gamma_b$  can be written as [43]

$$f(\gamma_b) = \frac{\gamma_b^{L-1}}{(L-1)! \bar{\gamma}_c^L} \exp\left(-\frac{\gamma_b}{\bar{\gamma}_c}\right), \quad (18)$$

where  $\bar{\gamma}_c$  is the average SNR per bit, defined as  $\bar{\gamma}_c = (E_b/N_0)E[\alpha_j^2] = (E_b/N_0)E[\alpha_l^2]$ ,  $j \neq l$ , and  $\sum_{l=1}^L E[\alpha_l^2] = 1$ .

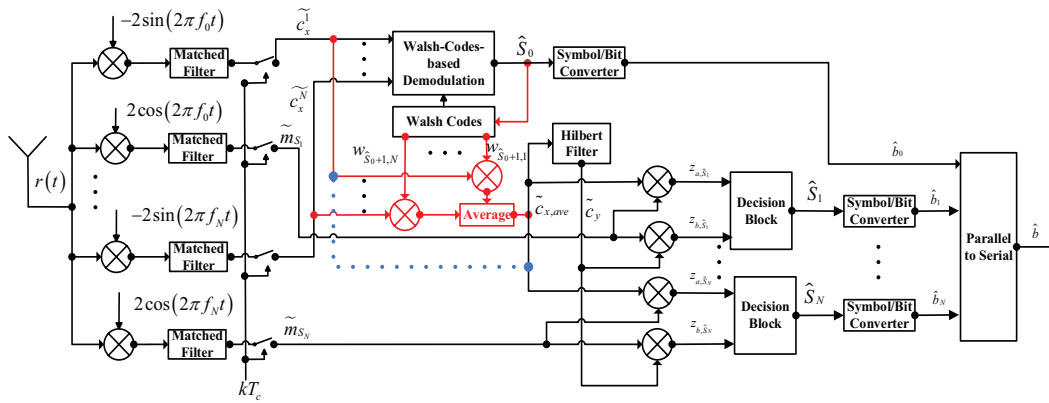


Fig. 3. The noise-reduction receiver structure of the proposed CIM-MC-M-DCSK system.

Finally, combining Eqs. (4), (15), (16) and (18), the average BER of the proposed system can be obtained as

$$\begin{aligned}
 P_b &= \int_0^\infty \left( \frac{\log_2 N}{\log_2 N + N \log_2 M} \times P_{b,MDCSK}(\gamma_b) \right. \\
 &\quad \left. + \frac{N \log_2 M}{\log_2 N + N \log_2 M} \times P_{b,CIM}(\gamma_b) \right) f(\gamma_b) d\gamma_b \\
 &= \frac{1}{R} \int_0^\infty \left( (\log_2 N) \times P_{b,MDCSK}(\gamma_b) \right. \\
 &\quad \left. + (N \log_2 M) \times P_{b,CIM}(\gamma_b) \right) f(\gamma_b) d\gamma_b. \quad (19)
 \end{aligned}$$

#### IV. NOISE REDUCTION AND HIERARCHICAL MODULATION FOR CIM-MC-M-DCSK SYSTEM

In this section, a noise-reduction scheme and a hierarchical-modulation scheme are developed for the proposed CIM-MC-M-DCSK system.

##### A. Noise-Reduction Scheme for the Proposed System

To obtain better BER performance we design a noise-reduction receiver for the proposed system, whose structure is shown in Fig. 3. In the CIM-MC-M-DCSK system, only a reference baseband signal is adopted to demodulate the quadrature baseband signals. In the proposed noise-reduction scheme, the noise of all reference baseband signals is averaged so as to reduce the negative effect [17], [18], [19]. The basic principle of the noise-reduction receiver is depicted as follows. First, the index bits are estimated. Based on the estimated index bits, the corresponding Walsh code is selected to be multiplied with the corresponding in-phase baseband signal, thus the estimated reference baseband signals are obtained. Finally, the estimated reference baseband signals are added and averaged to get the average reference baseband signal, which is used for demodulating the quadrature baseband signal from a subcarrier. More specifically, the expression of the average reference baseband signal can be written as

$$\begin{aligned}
 \tilde{c}_{x,ave} &= \frac{1}{N} \sum_{i=1}^N w_{\hat{S}_0+1,i} \tilde{c}_x^i \\
 &= \frac{1}{N} \sum_{i=1}^N w_{\hat{S}_0+1,i} \sum_{k=1}^{\beta} \left( \sum_{l=1}^L \alpha_l w_{S_0+1,i} c_{x-\tau_l} + n_{x,k}^i \right). \quad (20)
 \end{aligned}$$

According to such a noise-reduction scheme, one can derive the BER expression of the proposed noise-reduction CIM-MC-M-DCSK scheme. There are two possible cases when the demodulation error for the modulated bits happens.<sup>4</sup> In the first case, if the index symbol is not correctly estimated, Eq. (20) can be derived as

$$\tilde{c}_{x,ave} = \frac{1}{N} \sum_{i=1}^N w_{\hat{S}_0+1,i} n_{x,k}^i. \quad (21)$$

It can be easily seen from Eq. (21) that the modulated bits are not correctly estimated. Hence, the BER of the modulated bits are formulated as

$$P_{b,case1}(\gamma_b) = P_{b,CIM}(\gamma_b). \quad (22)$$

In the second case, the index symbol is correctly estimated. It is assumed that the BER of the M-DCSK modulation for the proposed noise-reduction CIM-MC-M-DCSK system is denoted as  $P_{ber}(\gamma_b)$ . The BER expression of the modulated bits is given by

$$P_{b,case2}(\gamma_b) = \left( 1 - P_{s,CIM}(\gamma_b) \right) P_{ber}(\gamma_b). \quad (23)$$

Because the index symbol is correctly detected, Eq. (20) can be modified to

$$\tilde{c}_{x,ave} = \sum_{k=1}^{\beta} \left( \sum_{l=1}^L \alpha_l c_{x-\tau_l} + \frac{1}{N} \sum_{i=1}^N w_{S_0+1,i} n_{x,k}^i \right). \quad (24)$$

According to Eq. (24), one can obtain the means and the variances of two elements in  $z_i$ , i.e.,  $E[z_{a,\hat{S}_i}] = a_{S_i} E_1 \sum_{l=1}^L \alpha_l^2$ ,  $E[z_{b,\hat{S}_i}] = b_{S_i} E_1 \sum_{l=1}^L \alpha_l^2$ , and  $Var[z_{a,\hat{S}_i}] = Var[z_{b,\hat{S}_i}] = \frac{N+1}{2N} E_1 N_0 \sum_{l=1}^L \alpha_l^2 + \frac{\beta N_0^2}{4N}$ , respectively. Hence, the instantaneous PDF conditioned on  $\gamma_b$  is the same as Eq. (11), where the expression of  $\gamma$  is changed to

$$\gamma = \frac{2R\gamma_b}{\sqrt{(N+1)R\gamma_b + N\beta}}. \quad (25)$$

<sup>4</sup>Differing from the proposed CIM-MC-M-DCSK system, the detections of the code-index modulation and M-DCSK modulation of the proposed noise-reduction CIM-MC-M-DCSK system are not independent, the error detection of the code-index modulation does affect the demodulation performance of the M-DCSK modulation.

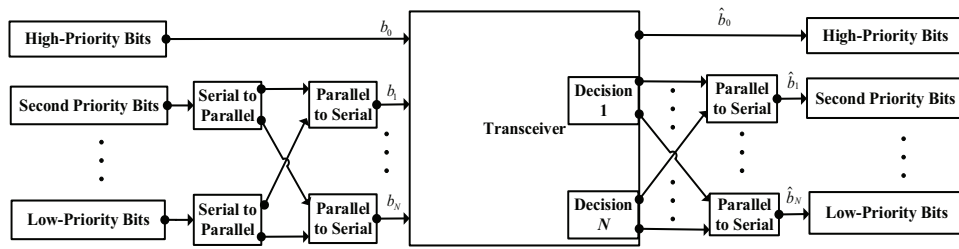


Fig. 4. A simple structure of the proposed hierarchical CIM-MC-M-DCSK system.

Substituting (11) and (25) into (16) (or (17)) yields the BER of the of  $M$ -DCSK modulation  $P_{ber}(\gamma_b)$ . Therefore, the overall BER of the proposed system with noise-reduction scheme becomes

$$P_b = \frac{1}{R} \int_0^\infty \left( (\log_2 N) \times P_{b,CIM}(\gamma_b) + (N \log_2 M) \times (P_{b,CIM}(\gamma_b) + P_{b,case2}(\gamma_b)) \right) f(\gamma_b) d\gamma_b. \quad (26)$$

### B. Hierarchical Modulation Scheme for the Proposed System

In practical short-range wireless-communication applications, the transmitted information bits usually have different levels of importance. To satisfy different QoS requirements for such transmitted information bits, a simple hierarchical CIM-MC-M-DCSK scheme is conceived, whose structure is illustrated in Fig. 4. It should be noted that the transceiver in Fig. 4 is identical to that in Fig. 1, where the  $M$ -DCSK modulation and the decision modules are replaced by the hierarchical  $M$ -DCSK modulation and decision modules in [14], respectively. To be specific, the index bits  $b_0$  have high priority and are transmitted through the CIM module, whereas the transmitted modulated bits  $b_i$  for the  $i$ -th subcarrier varying from second to low priority are transmitted through the hierarchical  $M$ -DCSK modulation module. Therefore, when compared with the hierarchical MC-M-DCSK system, the proposed hierarchical CIM-MC-M-DCSK system not only can obtain better performance but also can satisfy applications with high QoS requirements.

Here, we also carry out the BER derivation of the hierarchical CIM-MC-M-DCSK system.

To begin with, the BER expression of the transmitted index bits with high priority is given by

$$P_{b,High} = \int_0^\infty P_{b,CIM}(\gamma_b) f(\gamma_b) d\gamma_b. \quad (27)$$

Subsequently, the BER expressions of the transmitted modulated bits from second to low priority are summarized as follows. Exploiting Eq. (11), the CDF of the proposed hierarchical CIM-MC-MDCSK scheme is written as

$$F(\phi) = \int_{-\pi}^{\phi} \int_0^{+\infty} p(\varphi|\gamma_b) f(\gamma_b) d\gamma_b d\varphi, \quad -\pi < \phi < \pi. \quad (28)$$

In the high SNR region, Eq. (28) can be approximated as

$$F(\phi) \approx 0.5 - \int_0^{+\infty} Q\left(\frac{\gamma \sin \phi}{2}\right) f(\gamma_b) d\gamma_b, \quad -\pi < \phi < \pi, \quad (29)$$

where  $\gamma = \frac{2R}{\sqrt{2R}} \frac{\gamma_b}{\gamma_b + \beta}$ . Interested readers are referred to Appendix for more details of the derivation.

The average BERs for the second priority bit  $i_1$  and the third priority bit  $i_2$ , are respectively expressed as

$$P_b(4, \theta_1, i_1) = 1 - F(\theta_1) + F(-\pi + \theta_1), \quad (30)$$

$$P_b(4, \theta_1, i_2) = 1 - F\left(\frac{\pi}{2} - \theta_1\right) + F\left(-\frac{\pi}{2} + \theta_1\right), \quad (31)$$

Using Eqs. (30) and (31) and the recursive algorithm, the average BER for the  $(k+1)$ -th priority bit  $i_k$  ( $k < m$ ) can be calculated as

$$P_b(M, \theta, i_k) = \frac{1}{2} \left[ P_b\left(\frac{M}{2}, \theta_+, i_k\right) + P_b\left(\frac{M}{2}, \theta_-, i_k\right) \right], \quad (32)$$

where  $\theta_+ = [\pi/2 - \theta_1, \theta_2, \dots, \theta_{m-3}, \theta_{m-2} + \theta_{m-1}]$  and  $\theta_- = [\pi/2 - \theta_1, \theta_2, \dots, \theta_{m-3}, \theta_{m-2} - \theta_{m-1}]$ .

Moreover, the average BER of the low-priority bit  $i_m$  is given by

$$P_b(M, \theta, i_m) = \frac{1}{2^m} \left[ \sum_{i=1}^{2^{m-1}} \sum_{j=1}^{2^{m-1}} (-1)^j F(\mathbf{a}(j) - \Phi_0(i)) + \sum_{i=1}^{2^{m-1}} \sum_{j=1}^{2^{m-1}} (-1)^{j+1} F(\mathbf{a}(j) - \Phi_1(i)) \right], \quad (33)$$

where  $\mathbf{a}$  represents the angular positions of the decision boundaries of the low-priority bit,  $\Phi_0$  represents the angular positions of those symbols whose low-priority bit is 1, and  $\Phi_1$  represents the angular positions of those symbols whose low-priority bit is 0.

## V. NUMERICAL RESULTS AND DISCUSSIONS

In this section, we evaluate the BER performance of the proposed systems over AWGN as well as multipath Rayleigh fading channels. In simulation, the parameters of the multipath Rayleigh fading channel are set as follows:  $L = 3$ ,  $E[\alpha_1^2] = E[\alpha_2^2] = E[\alpha_3^2] = 1/3$ , and  $\tau_1 = 0$ ,  $\tau_2 = 2$  and  $\tau_3 = 5$ . Moreover, the spreading factors are set to 128 and 256 for both AWGN and multipath Rayleigh fading channels, respectively.

### A. Theoretical and Simulated BER Performance of the Proposed Systems

Figs. 5-8 shows the theoretical and simulated BER results of the proposed CIM-MC-M-DCSK system, and its noise-reduction counterpart (denoted by 'CIM-MC-MDCSK-NR' in

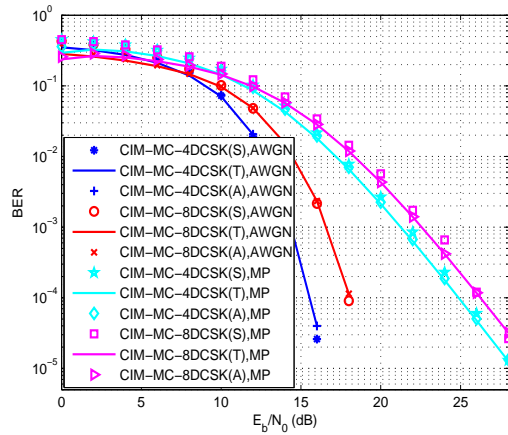


Fig. 5. Theoretical, approximated, and simulated BER results of the CIM-MC-M-DCSK system over AWGN and multipath Rayleigh fading channels.

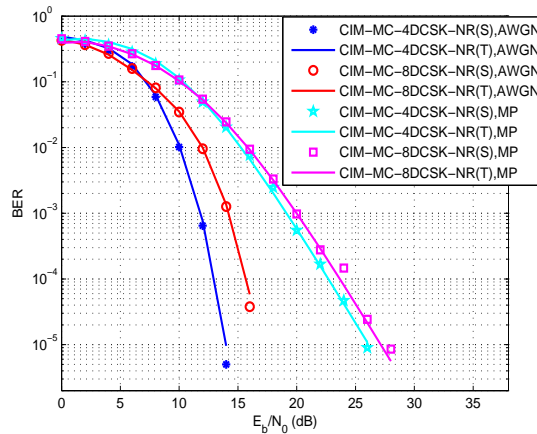


Fig. 6. Theoretical and simulated BER results of the CIM-MC-M-DCSK system with noise reduction over AWGN and multipath Rayleigh fading channels.

the figure) and hierarchical-modulation counterpart (denoted by ‘HCIM-MC-MDCSK’ in the figure) over AWGN and multipath Rayleigh fading channels, respectively, where ‘T’, ‘S’ and ‘A’ denote theoretical, simulated and approximated results, respectively, and ‘MP’ presents multipath Rayleigh fading channel. We assume that the order of Walsh code is  $N = 4$ . For a CIM-MC-M-DCSK system and its noise-reduction counterpart, we also assume that  $\theta = \pi/4$  for 4-DCSK and  $\theta = [\pi/4, \pi/8]$  for 8-DCSK. For hierarchical CIM-MC-M-DCSK system, we assume that  $\theta = \pi/3$  for hierarchical 4-DCSK and  $\theta = [\pi/4, \pi/15]$  for hierarchical 8-DCSK. Figs. 5-8 show that the simulated results are in good agreement with the theoretical results. Furthermore, Fig. 5 shows that the approximated results match well with the theoretical results in the high SNR region while the former only has a little difference compared with the latter in the low SNR region. For the noise-reduction and hierarchical-modulation CIM-MC-M-DCSK systems, one can make similar observations. Moreover, it can be observed that the BER performance of the CIM-MC-M-DCSK and its noise-reduction counterpart is deteriorated with the increase of  $M$ . In addition, referring to Figs. 7 and 8, the proposed hierarchical CIM-MC-M-DCSK system can

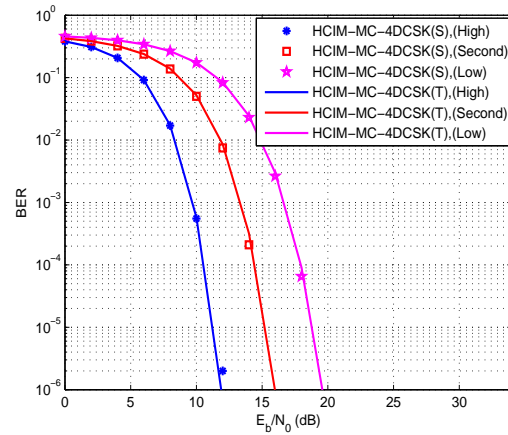


Fig. 7. Theoretical and simulated BER results of the hierarchical CIM-MC-M-DCSK system with priority vector  $\theta = \pi/3$  over an AWGN channel.

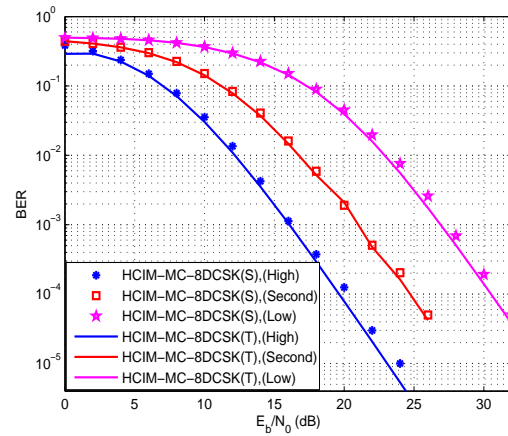
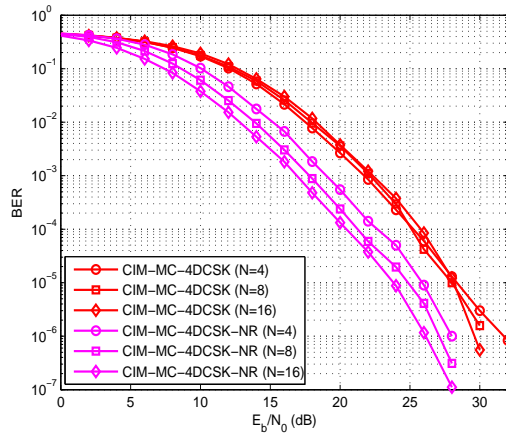


Fig. 8. Theoretical and simulated BER results of the hierarchical CIM-MC-M-DCSK system with priority vector  $\theta = [\pi/4, \pi/15]$  over a multipath Rayleigh fading channel.

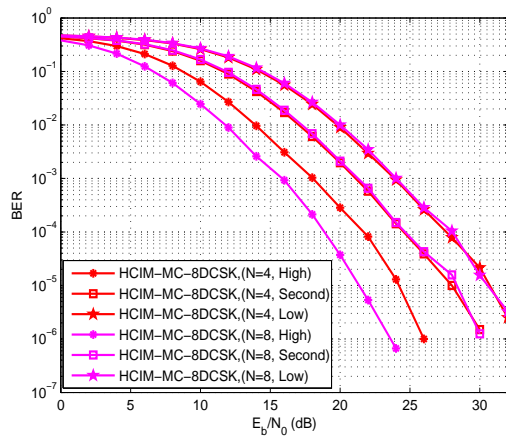
perfectly satisfy the QoS requirements for the bit streams that have different levels of importance.

### B. Effect of $N$ and $\beta$ on the System Performance

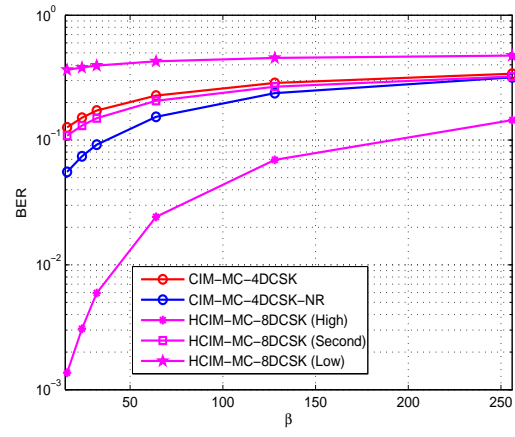
The effect of Walsh-code order  $N$  on the BER performance of the CIM-MC-M-DCSK system, its noise-reduction and hierarchical-modulation counterparts over a multipath Rayleigh fading channel are shown in Fig. 9, where  $\theta = \pi/4$  is used for hierarchical 4-DCSK and  $\theta = [\pi/4, \pi/15]$  used for hierarchical 8-DCSK. Fig. 9(a) shows that the BER of the CIM-MC-M-DCSK system is not improved with the increasing of  $N$ . However, as  $N$  increases, the noise-reduction CIM-MC-M-DCSK system can achieve an improved performance. For example, the noise-reduction CIM-MC-M-DCSK system with  $N = 8$  can accomplish a gain of about 1 dB with respect to that with  $N = 4$  at a BER of  $10^{-6}$ . In addition, it can be seen from Fig. 9(b) that the high-priority bits in the hierarchical CIM-MC-M-DCSK system with  $N = 8$  can achieve a 2-dB performance gain over that with  $N = 4$  while the performance of the second priority and low-priority bits is not improved as  $N$  increases. Furthermore, Fig. 10 shows the effect of  $\theta$  on the BER performance of the HCIM-MC-DCSK system over



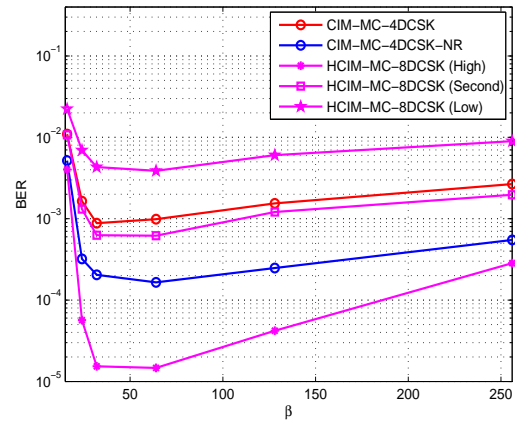
(a)



(b)



(a)



(b)

Fig. 9. BER performance of (a) the CIM-MC-M-DCSK system and its noise-reduction counterpart and (b) its hierarchical-modulation CIM-MC-M-DCSK system with different values of  $N$  over a multipath Rayleigh fading channel.

Fig. 11. BER performance of the CIM-MC-M-DCSK system, its noise-reduction scheme and its hierarchical-modulation scheme with different value of  $\beta$  (a) over AWGN at a bit SNR of 5 dB and (b) over multipath Rayleigh fading channel at a bit SNR of 20 dB.

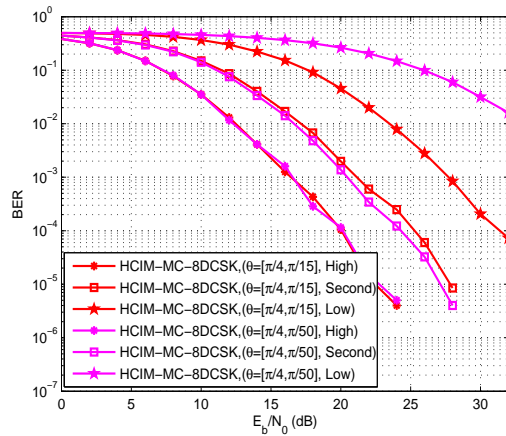


Fig. 10. BER performance of the hierarchical-modulation CIM-MC-M-DCSK system with different values of  $\theta$  over a multipath Rayleigh fading channel.

related to the value of  $\theta$  while the performance of the high-priority bits is independent of this parameter.

The effect of spreading factor  $\beta$  on the BER performance of the CIM-MC-M-DCSK system, its noise-reduction and hierarchical-modulation counterparts over AWGN and multipath Rayleigh fading channels is shown in Fig. 11, where  $\theta = [\pi/4, \pi/15]$  used for hierarchical 8-DCSK. It can be observed from Fig. 11(a) that the BER performance deteriorates as  $\beta$  increases, which is the same as the conventional DCSK systems. Referring to Fig. 11(b), the proposed system has an optimal value of  $\beta$  to obtain best BER performance. This phenomenon is due to the fact that the ISI is severe when spreading factor  $\beta$  is small. The ISI becomes negligible as  $\beta$  increases, thus the performance is improved. However, with increasing the spreading factor more noise is also involved as  $\beta$  further increases, which leads to a performance degradation.

### C. Comparison between the Proposed System and Existing Counterparts

To further verify the superiority of the proposed systems, we compare the BER performance of the proposed system

a multipath Rayleigh fading channel, where  $\theta = [\pi/4, \pi/15]$  and  $\theta = [\pi/4, \pi/50]$  are used. It can be observed that the performance of the second-priority and low-priority bits is

TABLE I  
COMPARISON FOR THE NUMBER OF THE TRANSMITTED BITS BETWEEN  
CIM-MC- $M$ -DCSK AND MC- $M$ -DCSK SYSTEMS.

System order	The number of the transmitted bits	
	MC- $M$ -DCSK	CIM-MC- $M$ -DCSK
$N = 4, M = 4$	8	10
$N = 4, M = 8$	12	14
$N = 4, M = 16$	16	18
$N = 8, M = 4$	16	19
$N = 8, M = 8$	24	27
$N = 8, M = 16$	32	35

with the MC- $M$ -DCSK system and its hierarchical-modulation scheme over a multipath Rayleigh fading channel.

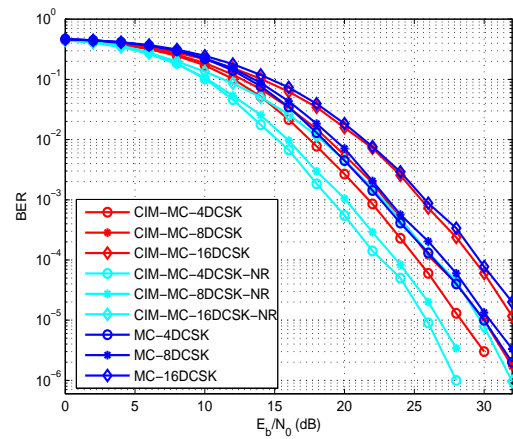
Table I compares the number of transmitted bits of the CIM-MC- $M$ -DCSK and MC- $M$ -DCSK systems.<sup>5</sup> It can be observed that the proposed CIM-MC- $M$ -DCSK system provides higher data rate compared with the conventional MC- $M$ -DCSK system under the same system order (i.e., under the same  $N$  and  $M$ ). Fig. 12 shows the BER curves of the CIM-MC- $M$ -DCSK, noise-reduction CIM-MC- $M$ -DCSK and MC- $M$ -DCSK systems over a multipath Rayleigh fading channel. From Fig. 12 (a) and (b), it can be seen that the proposed noise-reduction CIM-MC- $M$ -DCSK system can achieve the best BER performance among the three MC- $M$ -DCSK systems. For example, at a BER of  $10^{-5}$ , the noise-reduction CIM-MC-4-DCSK system can achieve 4-dB and 6.5-dB gains compared with the MC-4-DCSK system when  $N = 4$  and  $N = 8$ , respectively. Moreover, the CIM-MC- $M$ -DCSK system can accomplish better performance than that of the MC- $M$ -DCSK system under the same system order. Especially, at a BER of  $10^{-5}$ , the CIM-MC-16-DCSK system can achieve about 1-dB gain over the MC-16-DCSK system when  $N = 4, 8$ .

As a further insight, Fig. 13 shows the BER performance of the proposed hierarchical CIM-MC-4-DCSK and the hierarchical MC-4-DCSK systems over a multipath Rayleigh fading channel, where  $\theta = \pi/3$  and  $N = 4$  are used. It is shown that the hierarchical CIM-MC-4-DCSK system can provide better BER performance than that of the CIM-MC-4-DCSK system for any priority bits. For example, at a BER of  $10^{-5}$ , the high-priority bits of the hierarchical CIM-MC-4-DCSK system can achieve a 4-dB gain over the MC-4-DCSK system. In addition, one can observe that the second-priority bits of the hierarchical CIM-MC-4-DCSK system can achieve a 1-dB gain over the high-priority bits of the MC-4-DCSK system. Consequently, the hierarchical CIM-MC- $M$ -DCSK system can provide higher QoS and data rate with respect to the hierarchical MC- $M$ -DCSK system under the same system order and angle vector.

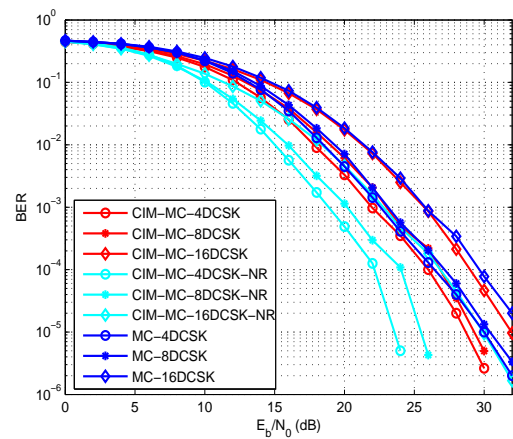
## VI. CONCLUSIONS

In this paper, we have proposed a new MC- $M$ -DCSK system with code index modulation, called CIM-MC- $M$ -DCSK system, in which the code index modulation and

<sup>5</sup>The number of the transmitted bits for the MC- $M$ -DCSK system can be calculated as  $N \log_2 M$ .



(a)



(b)

Fig. 12. BER performance of the CIM-MC- $M$ -DCSK, noise-reduction CIM-MC- $M$ -DCSK, MC- $M$ -DCSK and conventional DCSK systems over a multipath Rayleigh fading channel, where (a)  $N = 4$  and (b)  $N = 8$ .

$M$ -DCSK modulation are exploited in the reference signals and information-bearing signals, respectively. The proposed MC- $M$ -DCSK system not only inherits the low-complexity advantage of the conventional MC-DCSK system but also achieves better performance by using Walsh-codes-based index modulation. Furthermore, we have designed a noise-reduction scheme and a hierarchical-modulation scheme for the proposed CIM-MC- $M$ -DCSK system. In particular, the former scheme can significantly improve the BER performance, while the latter scheme can provide a more flexible QoS for the transmitted bits that have different levels of importance. In addition to the system design and optimization, we have derived the analytical BER expressions of the proposed systems over AWGN and multipath fading channels. Both the theoretical analyses and simulation results have demonstrated that the proposed CIM-MC- $M$ -DCSK and its hierarchical-modulation systems can achieve better performance over the existing MC- $M$ -DCSK and its hierarchical-modulation systems, respectively. Thanks to the excellent performance and simple implementation, the proposed CIM-MC- $M$ -DCSK system appears to be an outstanding candidate for the low-cost and low-power short-range

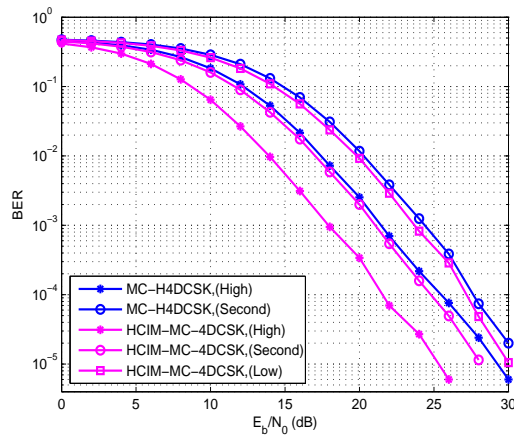


Fig. 13. BER performance of the hierarchical CIM-MC-4-DCSK and the hierarchical MC-4-DCSK systems over a multipath Rayleigh fading channel.

wireless-communication applications.

#### APPENDIX DERIVATION OF (17) AND (29)

To obtain Eqs. (17) and (29), we first derive an approximated closed-form expression for the integration of  $p(\varphi|\gamma_b)$ , i.e.,

$$F_e = \int_a^b \left[ \frac{1}{2\pi} \exp\left(\frac{-\gamma^2}{8}\right) + \frac{\gamma \cos \varphi}{2\sqrt{2\pi}} \exp\left(\frac{-\gamma^2 \sin^2 \varphi}{8}\right) Q\left(\frac{-\gamma \cos \varphi}{2}\right) \right] d\varphi. \quad (34)$$

Exploiting  $Q(-x) = 1 - Q(x)$ , Eq. (34) can be expanded to

$$\begin{aligned} F_e &= \int_a^b \frac{1}{2\pi} \exp\left(\frac{-\gamma^2}{8}\right) d\varphi \\ &\quad - \int_a^b \frac{\gamma \cos \varphi}{2\sqrt{2\pi}} \exp\left(\frac{-\gamma^2 \sin^2 \varphi}{8}\right) Q\left(\frac{\gamma \cos \varphi}{2}\right) d\varphi \\ &\quad + \int_a^b \frac{\gamma \cos \varphi}{2\sqrt{2\pi}} \exp\left(\frac{-\gamma^2 \sin^2 \varphi}{8}\right) d\varphi \\ &= F_{e1} + F_{e2} + F_{e3}. \end{aligned} \quad (35)$$

One can easily calculate  $F_{e1}$  as

$$F_{e1} = \int_a^b \frac{1}{2\pi} \exp\left(\frac{-\gamma^2}{8}\right) d\varphi = \frac{b-a}{2\pi} \exp\left(\frac{-\gamma^2}{8}\right). \quad (36)$$

Utilizing the approximated expression of  $Q$  function, i.e.,  $Q(x) \approx \frac{1}{x\sqrt{2\pi}} \exp\left(-\frac{x^2}{2}\right)$ , for large  $x$ , one has

$$\begin{aligned} F_{e2} &= - \int_a^b \frac{\gamma \cos \varphi}{2\sqrt{2\pi}} \exp\left(\frac{-\gamma^2 \sin^2 \varphi}{8}\right) Q\left(\frac{\gamma \cos \varphi}{2}\right) d\varphi \\ &\approx - \frac{b-a}{2\pi} \exp\left(\frac{-\gamma^2}{8}\right). \end{aligned} \quad (37)$$

Based on Eqs. (36) and (37) and let  $u = \frac{\gamma \sin(\varphi)}{2}$ , Eq. (35) can be reduced to

$$\begin{aligned} F_e &\approx \int_a^b \frac{\gamma \cos \varphi}{2\sqrt{2\pi}} \exp\left(\frac{-\gamma^2 \sin^2 \varphi}{8}\right) d\varphi \\ &= \frac{1}{\sqrt{2\pi}} \int_{\frac{\gamma \sin(a)}{2}}^{\frac{\gamma \sin(b)}{2}} \exp\left(-\frac{u^2}{2}\right) du. \end{aligned} \quad (38)$$

Suppose  $a = -\pi/M$  and  $b = \pi/M$ , Eq. (38) becomes

$$\begin{aligned} F_e &\approx \frac{2}{\sqrt{2\pi}} \int_0^{\frac{\gamma \sin(\frac{\pi}{M})}{2}} \exp\left(-\frac{u^2}{2}\right) du \\ &= 1 - 2Q\left(\frac{\gamma \sin(\frac{\pi}{M})}{2}\right). \end{aligned} \quad (39)$$

Likewise, assume  $a = -\pi$  and  $b = \phi$ , Eq. (38) becomes

$$F_e \approx 0.5 - Q\left(\frac{\gamma \sin \phi}{2}\right). \quad (40)$$

As a consequence, substituting (39) into (16) yields the closed-form expression (17). Moreover, substituting (40) into (28) obtains the closed-form expression (29).

#### REFERENCES

- [1] M. P. Kennedy, G. Kolumban, G. Kis, and Z. Jako, "Performance evaluation of FM-DCSK modulation in multipath environments," *IEEE Trans. Circuits Syst. I, Reg. Papers*, vol. 47, no. 12, pp. 1702-1711, Dec. 2000.
- [2] Y. Fang, G. Han, P. Chen, F. C. M. Lau, G. Chen, and L. Wang, "A survey on DCSK-based communication systems and their application to UWB scenarios," *IEEE Commun. Surveys & Tutorials*, vol. 18, no. 3, pp. 1804-1837, Third Quarter 2016.
- [3] G. Cai, Y. Fang, G. Han, J. Xu, and G. Chen, "Design and analysis of relay-selection strategies for two-way relay network-coded DCSK systems," *IEEE Trans. Veh. Technol.*, vol. 67, no. 2, pp. 1258-1271, Feb. 2018.
- [4] G. Kaddoum, H. V. Tran, L. Kong, and M. Atallah, "Design of simultaneous wireless information and power transfer scheme for short reference DCSK communication systems," *IEEE Trans. Commun.*, vol. 65, no. 1, pp. 431-443, Jan. 2017.
- [5] F. J. Escribano, G. Kaddoum, A. Wagemakers, and P. Giard, "Design of a new differential chaos-shift-keying system for continuous mobility," *IEEE Trans. Commun.*, vol. 64, no. 5, pp. 2066-2078, May 2016.
- [6] G. Kaddoum and N. Tadayon, "Differential chaos shift keying: A robust modulation scheme for power-line communications," *IEEE Trans. Circuits Syst. II, Exp. Briefs*, vol. 64, no. 1, pp. 31-35, Jan. 2017.
- [7] Y. Fang, L. Wang, X. Jing, P. Chen, G. Chen, and W. Xu, "Design and analysis of a DCSK-ARQ/CARQ system over multipath fading channels," *IEEE Trans. Circuits Syst. I, Reg. Papers*, vol. 62, no. 6, pp. 1637-1647, Jun. 2015.
- [8] W. Xu, L. Wang, and G. Chen, "Performance analysis of the CS-DCSK/BPSK communication system," *IEEE Trans. Circuits Syst. I, Reg. Papers*, vol. 61, no. 9, pp. 2624-2633, Sep. 2014.
- [9] Y. Fang, J. Xu, L. Wang, and G. Chen, "Performance of MIMO relay DCSK-CD systems over Nakagami fading channels," *IEEE Trans. Circuits Syst. I, Reg. Papers*, vol. 60, no. 3, pp. 757-767, Mar. 2013.
- [10] H. Yang, W. K. S. Tang, G. Chen, and G. Jiang, "System design and performance analysis of orthogonal multi-level differential chaos shift keying modulation scheme," *IEEE Trans. Circuits Syst.-I*, vol. 63, no. 1, pp. 146-156, Jan. 2016.
- [11] Z. Galias and G. M. Maggio, "Quadrature chaos-shift keying: Theory and performance analysis," *IEEE Trans. Circuits Syst. I, Fundam. Theory Appl.*, vol. 48, no. 12, pp. 1510-1519, Dec. 2001.
- [12] G. Cai, Y. Fang, G. Han, F. C. M. Lau, and L. Wang, "A square-constellation-based  $M$ -ary DCSK communication system," *IEEE Access*, vol. 4, pp. 6295-6303, 2016.
- [13] G. Kaddoum, E. Soujeri, and Y. Nijssure, "Design of a short reference noncoherent chaos-based communication systems," *IEEE Trans. Commun.*, vol. 64, no. 2, pp. 680-689, Feb. 2016.

- [14] L. Wang, G. Cai, and G. Chen, "Design and performance analysis of a new multiresolution  $M$ -ary differential chaos shift keying communication system," *IEEE Trans. Wireless Commun.*, vol. 14, no. 9, pp. 5197-5208, Sept. 2015.
- [15] G. Cai, Y. Fang, G. Han, L. Wang, and G. Chen, "A new hierarchical  $M$ -ary DCSK system: Design and analysis," *IEEE Access*, vol. 5, no. 1, pp. 17414-17424, Dec. 2017
- [16] G. Cai, Y. Fang, G. Han, "Design of an adaptive multiresolution  $M$ -ary DCSK system," *IEEE Commun. Lett.*, vol. 17, no. 1, pp. 60-63, Jan. 2017.
- [17] G. Kaddoum and E. Soujeri, "NR-DCSK: A noise reduction differential chaos shift keying system," *IEEE Trans. Circuits Syst. II, Express Briefs*, vol. 63, no. 7, pp. 648-652, Jul. 2016.
- [18] G. Kolumban, Z. Jako, and M. P. Kennedy, "Enhanced version of DCSK and FM-DCSK data transmission systems," in *Proc. IEEE ISCAS*, Orlando, FL, USA, Jul. 1999, pp. 475-478.
- [19] G. Kolumban, M. P. Kennedy, Z. Jako, and G. Kis, "Chaotic communications with correlator receivers: Theory and performance limits," *Proc. IEEE*, vol. 90, no. 5, pp. 711-732, May 2002.
- [20] W. Xu, L. Wang, and G. Kolumban, "A novel differential chaos shift keying modulation scheme," *In. J. of Bifurcations and Chaos*, vol. 21, no. 3, pp. 799-814, Mar. 2011.
- [21] W. Xu, L. Wang, and G. Kolumban, "A new data rate adaption communications scheme for code-shifted differential chaos shift keying modulation," *In. J. of Bifurcations and Chaos*, vol. 22, no. 8, pp. 1-9, Sept. 2012.
- [22] G. Kaddoum, F. Gagnon, and F.-D. Richardson, "Design and analysis of a multi-carrier differential chaos shift keying communication system," *IEEE Trans. Commun.*, vol. 61, no. 8, pp. 3281-3291, Aug. 2013.
- [23] G. Kaddoum, "Design and performance analysis of a multiuser OFDM based differential chaos shift keying communication system," *IEEE Trans. Commun.*, vol. 64, no. 1, pp. 249-260, Jan. 2016.
- [24] H. Yang, G. Jiang, and J. Duan, "Phase-separated DCSK: A simple delay component-free solution for chaotic communications," *IEEE Trans. Circuits Syst.-II, Express Briefs*, vol. 61, no. 12, pp. 967-971, Dec. 2014.
- [25] E. Basar, "Orbital angular momentum with index modulation," *IEEE Trans. Wireless Commun.*, vol. 17, no. 3, pp. 2029-2037, Mar. 2018.
- [26] M. Wen, Q. Li, E. Basar, and W. Zhang, "Generalized multiple-mode OFDM with index modulation," *IEEE Trans. Wireless Commun.*, vol. 17, no. 10, pp. 6531-6543, Oct. 2018.
- [27] E. Basar, M. Wen, R. Mesleh, M. Di Renzo, Y. Xiao, H. Haas, "Index modulation techniques for next-generation wireless networks," *IEEE Access*, vol. 5, no. 1, pp. 16693-16746, Sep. 2017.
- [28] G. Kaddoum, Y. Nijsure, and H. Tran, "Generalized code index modulation technique for high-data-rate communication systems," *IEEE Trans. Veh. Technol.*, vol. 65, no. 9, pp. 7000-7009, Sep. 2016.
- [29] M. Wen, E. Basar, Q. Li, B. Zheng, and M. Zhang, "Multiple-mode orthogonal frequency division multiplexing with index modulation," *IEEE Trans. Commun.*, vol. 65, no. 9, pp. 3892-3906, Sept. 2017.
- [30] E. Basar, U. Aygolu, E. Panayirci, and H. V. Poor, "Orthogonal frequency division multiplexing with index modulation," *IEEE Trans. Signal Process.*, vol. 61, no. 22, pp. 5536-5549, Nov. 2013.
- [31] M. Wen, B. Ye, E. Basar, Q. Li, and F. Ji, "Enhanced orthogonal frequency division multiplexing with index modulation," *IEEE Trans. Wireless Commun.*, vol. 16, no. 7, pp. 4786-4801, Jul. 2017.
- [32] M. Wen, Y. Zhang, J. Li, E. Basar, and F. Chen, "Equiprobable subcarrier activation method for OFDM with index modulation," *IEEE Communications Letters*, vol. 20, no. 12, pp. 2386-2389, Dec. 2016.
- [33] Q. Li, M. Wen, E. Basar, and F. Chen, "Index modulated OFDM spread spectrum," *IEEE Trans. Wireless Commun.*, vol. 17, no. 4, pp. 2360-2374, Apr. 2018.
- [34] G. Kaddoum, M. F. A. Ahmed, and Y. Nijsure, "Code index modulation: A high data rate and energy efficient communication system," *IEEE Commun. Lett.*, vol. 19, no. 2, pp. 175-178, Feb. 2015.
- [35] W. Hu, L. Wang, and G. Kaddoum, "Design and performance analysis of a differentially spatial modulated chaos shift keying modulation system," *IEEE Trans. Circuits Syst. II, Exp. Briefs*, vol. 64, no. 11, pp. 1302-1306, Nov. 2017.
- [36] A. Kumar and P. R. Sahu, "Performance analysis of spatially modulated differential chaos shift keying modulation," *IET Commun.*, vol. 11, no. 6, pp. 905-909, Apr. 2017.
- [37] W. Xu, Y. Tan, F. C. M. Lau, and G. Kolumban, "Design and optimization of differential chaos shift keying scheme with code index modulation," *IEEE Trans. Commu.*, vol. 66, no. 5, pp. 1970-1980, May 2018.
- [38] W. Xu, T. Huang, and L. Wang, "Code-shifted differential chaos shift keying with code index modulation for high data rate transmission," *IEEE Trans. Commu.*, vol. 65, no. 10, pp. 4285-4294, Oct. 2017.
- [39] Y. Tan, W. Xu, T. Huang, and L. Wang, "A multilevel code shifted differential chaos shift keying scheme with code index modulation," *IEEE Trans. Circuits Syst. II, Exp. Briefs*, vol. 65, no. 11, pp. 1743-1747, Nov. 2018.
- [40] M. Herceg, G. Kaddoum, D. Vranjes, and E. Soujeri, "Permutation index DCSK modulation technique for secure multi-user high-data-rate communication systems," *IEEE Trans. Veh. Technol.*, vol. 67, no. 4, pp. 2997-3011, Apr. 2018.
- [41] G. Cheng, L. Wang, W. Xu, and G. Chen, "Carrier index differential chaos shift keying modulation," *IEEE Trans. Circuits Syst. II, Exp. Briefs*, vol. 64, no. 8, pp. 907-911, Aug. 2017.
- [42] G. Cheng, L. Wang, Q. Chen, G. Chen, "Design and performance analysis of generalised carrier index  $M$ -ary differential chaos shift keying modulation," *IET Commu.*, vol. 12, no. 11, pp. 1324-1331, May. 2018.
- [43] J. G. Proakis and M. Salehi, *Digital Communications*, McGraw-Hill, 2007.



**Guofa Cai** (M'17) received the B.Sc. degree in communication engineering from Jimei University, Xiamen, China, in 2007, the M.Sc. degree in circuits and systems from Fuzhou University, Fuzhou, China, in 2012, and the Ph.D. degree in communication engineering from Xiamen University, Xiamen, China, in 2015. In 2017, he was a Research Fellow at the School of Electrical and Electronic Engineering, Nanyang Technological University, Singapore. He is currently an Associate Professor with the School of Information Engineering, Guangdong University of Technology, China. His primary research interests include information theory and coding, spread-spectrum modulation, wireless body area networks, and Internet of Things.



**Yi Fang** (M'15) received the B.Sc. degree in electronic engineering from East China Jiaotong University, China, in 2008, and the Ph.D. degree in communication engineering, Xiamen University, China, in 2013. From May 2012 to July 2012, He was a Research Assistant in electronic and information engineering, Hong Kong Polytechnic University, Hong Kong. From September 2012 to September 2013, he was a Visiting Scholar in electronic and electrical engineering, University College London, UK. From February 2014 to February 2015, he was a Research Fellow at the School of Electrical and Electronic Engineering, Nanyang Technological University, Singapore. He is currently an Associate Professor at the School of Information Engineering, Guangdong University of Technology, China. His research interests include information and coding theory, LDPC/protograph codes, spread-spectrum modulation, and cooperative communications. He is an Associate Editor of IEEE Access.



**Jinming Wen** is a full professor in the College of Information Science and Technology and the College of Cyber Security, Jinan University, Guangzhou. He received his Bachelor degree in Information and Computing Science from Jilin Institute of Chemical Technology, Jilin, China, in 2008, his M.Sc. degree in Pure Mathematics from the Mathematics Institute of Jilin University, Jilin, China, in 2010, and his Ph.D degree in Applied Mathematics from McGill University, Montreal, Canada, in 2015. He was a postdoctoral research fellow at Laboratoire LIP (from March 2015 to August 2016), University of Alberta (from September 2016 to August 2017) and University of Toronto (from September 2017 to August 2018). He has been a full professor in Jinan University, Guangzhou since September 2018. His research interests are in the areas of lattice reduction and sparse recovery. He has published more than 40 papers in top journals (including Applied and Computational Harmonic Analysis, IEEE Transactions on Information Theory/ Signal Processing/Wireless Communications) and conferences. He is an Associate Editor of IEEE Access.



**Shahid Mumtaz** is an ACM Distinguished speaker, IEEE Senior member, EiC of IET “journal of Quantum communication” Vice Chair: Europe/Africa Region-IEEE ComSoc: Green Communications & Computing society and Vice-chair for IEEE standard on P1932.1: Standard for Licensed/Unlicensed Spectrum Interoperability in Wireless Mobile Networks. He has more than 12 years of wireless industry/academic experience. He has received his Master and Ph.D. degrees in Electrical & Electronic Engineering from Blekinge Institute of Technology,

Sweden, and University of Aveiro, Portugal in 2006 and 2011, respectively. He has been with Instituto de Telecomunicações since 2011 where he currently holds the position of Auxiliary Researcher and adjunct positions with several universities across the Europe-Asian Region. He is also a visiting researcher at Nokia Bell labs. He is the author of 4 technical books, 12 book chapters, 150+ technical papers in the area of mobile communications.



**Yang Song** received the B.Eng. degree in communication engineering from Zhejiang University City College, Hangzhou, China, in 2007, and the M.Eng. and Ph.D. degrees in electronic and information engineering from The Hong Kong Polytechnic University, Hong Kong, in 2008 and 2013, respectively. He was a Research Associate with The Hong Kong Polytechnic University until 2014. From 2014 to 2016, he was a Post-Doctoral Research Associate with the Universität Paderborn, Paderborn, Germany. Since 2016, he has been a Research Fellow

with Nanyang Technological University, Singapore. His current research interests include space-time signal processing. He is an Associate Editor of IET Signal Processing.



**Valerio Frascolla** received the M.Sc. and the Ph.D. degree in electronic engineering.

He is Director of research and innovation at Intel, Neubiberg, Germany. He had been working in different roles at Ancona University, Comneon, and Infineon. He has expertise in mobile terminals system architecture, requirements management, standards bodies attendance (3GPP, ETSI, and IEEE), and project and program management. He serves as coach and mentor with Intel, as well as in European projects (Fashion Fusion, WEARSustain). He acts

as facilitator of innovation activities using agile methodologies (CSM- and CSPO-certified). He has authored 70+ peer-reviewed publications. His main research interest is 5G system design with a focus on spectrum management, mm-waves, and MEC technologies.

Dr. Frascolla currently participates in several international research projects serving as consortium lead for business, standardization, innovation and exploitation matters, and organizing special sessions, workshops and panels at international conferences (VTC, EUCNC, WCNC, EUCAP, EUSIPCO, COCORA, EWSN, DySPAN, and ISWCS).